

Effect Of The Pressure On The Properties Of Oxygen-Containing Silicon Single Crystals

Abdumajid Turaev*, G'anijon Raxmonov, Azim Soatov, Rasul Burxanov, Omadbek Rayimjonov, Noiba Batirova

Center for the Development of Nanotechnology at the National University of Uzbekistan named after Mirzo Ulugbek

National University of Uzbekistan named after Mirzo Ulugbek

Abstract: It is known[1] that in silicon single crystals grown by the Czochralski method, the oxygen content can be controlled within $(2 - 8) \times 10^{17} \text{ cm}^{-3}$. In crystals grown by the FZ method (the crucible-less floating zone technique or "floating zone" method), both in vacuum and in the inert gas atmosphere, the oxygen content is less than $3 \times 10^{16} \text{ cm}^{-3}$. Hence, it is clear why the properties of silicon with oxygen content in the range $3 \times 10^{16} - 2 \times 10^{17} \text{ cm}^{-3}$ are least studied.

Keywords: silicon, oxygen

It is known[1] that in silicon single crystals grown by the Czochralski method, the oxygen content can be controlled within $(2 - 8) \times 10^{17} \text{ cm}^{-3}$. In crystals grown by the FZ method (the crucible-less floating zone technique or "floating zone" method), both in vacuum and in the inert gas atmosphere, the oxygen content is less than $3 \times 10^{16} \text{ cm}^{-3}$. Hence, it is clear why the properties of silicon with oxygen content in the range $3 \times 10^{16} - 2 \times 10^{17} \text{ cm}^{-3}$ are least studied.

It has been experimentally established that the oxygen concentration in silicon crystals varies depending on the growth conditions: the pulling speed, the rotation speed of the crystal and crucible, the composition of the melt, the growing atmosphere and the pressure of the inert gas [2,3]. The specified nominal oxygen concentration within the above limits can be provided in one of the following ways: by choosing the ratio of the contact surface area of the crucible to the open evaporation surface; by continuous feeding of the melt from which the crystal grows; by acting coaxially with the axis of crystal growth with a constant magnetic field, etc.

As noted above, many factors, including the degree of mixing of the melt, are controlling factors of the oxygen content in single crystals. When the crystal and the crucible rotate towards each other, the oxygen concentration increases with an increase in the diameter of the crystal and the speed of its rotation [4].

An increase in the rotation frequency of the crucible to 20 min^{-1} leads to a decrease in oxygen concentration by almost an order of magnitude [3].

When rotating long single crystals (1 - 1.5 m), the oxygen concentration in them can be reduced in the case of a monotonous increase in the crystal rotation frequency from $3 - 6 \text{ min}^{-1}$ at the beginning of the process to $25 - 30 \text{ min}^{-1}$ at the end. Moreover, the increase in the rotation speed of the crystal for every 10 cm of its length should be $0.5 - 2 \text{ min}^{-1}$, and the rotation frequency of the crucible is maintained constant throughout the process. In addition to reducing the oxygen concentration to a level of $4 \times 10^{17} \text{ cm}^{-3}$, the use of this technique ensures the uniform distribution of oxygen along the length of the single crystal.

A similar effect is also provided by the periodic shutdown of the crucible rotation within the duration of the on and off periods from 1 to 15 seconds []. In this case, the steady flows in the melt and at the melt-crucible boundary are periodically disrupted, which leads to a periodic intensification of crucible dissolution and melt oxygen supply, compensating for a decrease in its concentration towards the end of the crystal due to segregation.

Using the method of calculating the material balance of silicon and quartz to determine the solubility of quartz in a silicon melt, it was found that the main contribution to reducing the mass of the crucible and silicon loading is made by the interaction of the melt with quartz, accompanied by the formation and removal of SiO_2 , according to the reaction:



Having data on the decrease in the mass of silicon and quartz during their interaction at the crystallization temperature, it is possible to calculate with a fairly good approximation the rate of dissolution of quartz by

silicon melt as the ratio of the mass of quartz reacting with the melt from a unit surface of the crucible per unit time.

When studying the effect of alloying impurity (P, B, Sb) on the dissolution rate of quartz crucibles, it was found that the nature of the dependence of the quartz dissolution rate on pressure for cases of alloying the melt with boron or phosphorus is identical. However, the absolute values of the quartz dissolution rate are higher in a melt containing phosphorus, and for both cases decrease with a decrease in the degree of alloying of the silicon melt. The differences in the dissolution rates in unalloyed and alloyed melts are explained by an increase in viscosity in alloyed melts, which leads to a decrease in the intensity of convection flows and an increase in temperature on the crucible wall and, accordingly, an increase in the dissolution rate of the crucible. When studying the distribution of oxygen along the length of a single crystal from the type of alloying impurity, it was found that the oxygen concentration along the length of single crystals decreases from the upper to the lower end of the ingot and that this dependence is more pronounced in single crystals doped with phosphorus. The latter is explained by the greater affinity of phosphorus to oxygen compared to boron.

The oxygen concentration in silicon single crystals increases with increasing pressure in the chamber. At the same pressure in the chamber, the oxygen concentration is higher in single crystals grown with lower argon consumption. The implementation of the growing process in the area of low pressures in the chamber (0.13 - 0.76 kPa) and at high argon flow rates (more than $25 \times 10^5 \text{ cm}^3/\text{s}$) makes it possible to obtain a uniform distribution and oxygen concentration approaching the values for single crystals grown in vacuum. The uniform oxygen distribution in this case along the length of the single crystal is due to the fact that the thickness of the dynamic boundary layer above the surface of the melt remains practically constant throughout the growing process, i.e., the process proceeds at a constant rate of evaporation of SiO. In the case of low argon consumption, as the melt decreases, the SiO discharge deteriorates due to the shielding of the area above the melt from the argon intake by the side surface of the crucible. As a result, the thickness of the boundary layer increases, the evaporation of SiO from the melt worsens and the reaction between the silicon melt and the crucible slows down.

The influence of magnetic fields on the content and distribution of background impurities in Si crystals is manifested due to the effect on free convective flows in the melt, which leads to a change in the rate of quartz dissolution and oxygen transfer to the crystallization front. When a magnetic field is applied, free convection in the melt is suppressed, the temperature stabilizes, and decreases near the interface, and increases in the volume of the melt. In this case, the mass transfer mechanism in the melt changes. The velocity of the vertical flow directed to the interface decreases in the presence of a magnetic field, which leads to a drop in temperature in this area and a decrease in the interface concavity. This leads to a change in the pattern of growth bands that exists in crystals grown without a magnetic field, and is mainly due to the ratio of the speeds of ingot pulling and crucible rotation. The application of a magnetic field completely eliminates bands with a long period (0.25 - 0.5 mm) and there is a significant weakening of the impurity bands with a step of 20 microns. An example of the influence of a magnetic field on the content and distribution of background impurities of oxygen and carbon is shown in Fig. 6. Using a magnetic field in combination with the rotation of a crystal and a quartz crucible with a melt, it is easy to control the thermal field in the melt, and therefore ensure the necessary of interstitial oxygen concentrations in silicon crystals. In a magnetic field, it is possible to grow Si single crystals with a given oxygen content in wide ranges from $(4 - 5) \times 10^{17}$ to $(9 - 18) \times 10^{17} \text{ cm}^{-3}$.

The application of the continuous feeding method in the Czochralski process makes it possible to eliminate the instabilities of the growth kinetics, primarily due to changes in the melt volume during ingot growth. This makes it possible to reduce the spread in the distribution of impurities along the length of the ingot, which in crystals grown from a load of 30 - 60 kg, with an effective distribution coefficient of 0.3 - 0.5, reaches 30 - 50% of the required nominal value. This spread can be reduced by growing single crystals from small constant volumes of the melt. When free convection is weakened at the same time, the oxygen concentration spread decreases as a result of a decrease in temperature fluctuations near the crystal-melt interface.

It is known [2,3] that silicon single crystals obtained by both the Czochralski method and zone melting contain a significant number of oxygen atoms ($\sim 10^{18} \text{ cm}^{-3}$) and carbon ($\sim 10^{17} \text{ cm}^{-3}$), which are mainly in an electrically inactive state. At the same time, various external influences, such as pressure, heat treatment, irradiation with ionizing and high-energy particles, necessary both for the production of semiconductor

structures and inevitable during their operation, lead to the formation of a number of electrically active centers involving oxygen and carbon atoms, which play a decisive role in the degradation of silicon parameters and devices based on it based on. Along with such traditional types of external influences as lighting, heat treatment and irradiation with ionizing particles, in recent years there has been increased interest in studying the effect of high pressures on the properties of semiconductors and, in particular, the nature of the residual effects of this effect.

In work [2] the behavior of oxygen atoms before and after the all-round pressure (ARP) $P = 60 \div 80$ kbar in the temperature range $600 \div 800^\circ\text{C}$ was studied. The authors point out that as a result of plastic deformation of silicon single crystals under pressure $P = 70$ kbar and a temperature of 800°C , all optically active oxygen passes into an optically inactive state, as a result of which the absorption peak at 9.1 microns completely disappears, and after thermal annealing at 1100°C , it is restored within 5-10 seconds. The results of the conducted studies have shown that the introduction of vanadium atoms into n-Si leads to a slight change in the resistivity value, regardless of whether the initial samples passed the preliminary a high temperature annealing (HTA) or not. In the samples of p-Si<V> that passed the preliminary HTA, there is a significant increase in resistivity, and the increase is 2 - 3 times less than in the samples of p-Si<V> that did not pass the preliminary HTA).

It is also known [4] that during HTA at $T = 1100^\circ\text{C}$, precipitation of oxygen atoms occurs, that is, free interstitial oxygen passes into the second phase with the formation of SiO_2 particles. Some vanadium atoms, when introduced into pre-heat-treated silicon, apparently settle on SiO_2 clusters, as a result of which they probably lose their electrical activity. This probably explains the difference in the change in the value of ρ in the p-Si<V> samples with and without preliminary HTA. It should be added that preliminary studies conducted using capacitance spectroscopy have shown that there is a difference in the concentration of deep levels associated with vanadium atoms in Si with and without preliminary HTA.

Since there is no other information in print about the mechanisms of such transformations, we have conducted studies of residual effects after all-round hydrostatic pressure of the initial and nickel- and gadolinium-doped silicon samples. Figure 1 shows an installation, an industrial hydraulic press DO-138B for obtaining high pressure using an industrial high-pressure chamber for the synthesis of superhard materials such as lentils and toroids. Silver chloride powders were used as a working material for obtaining high pressure in lentils.

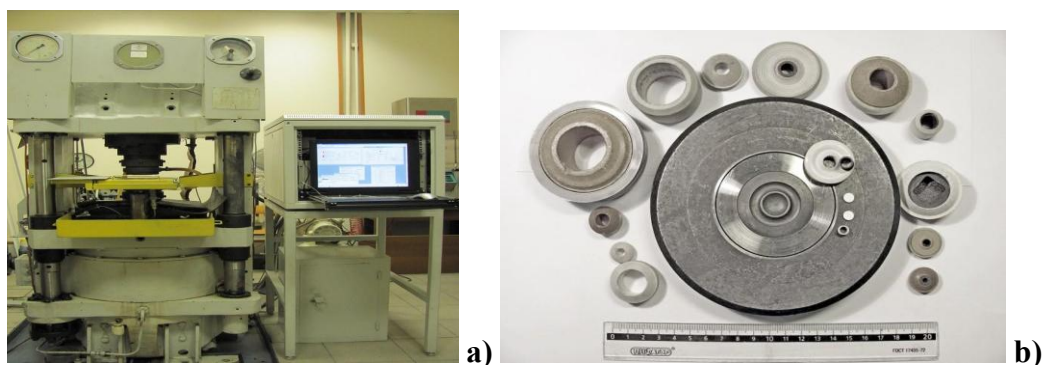


Fig. 1 a)- Industrial hydraulic press DO-138B for the synthesis of superhard materials with a force of 630 tons, b) industrial high-pressure chambers for the synthesis of superhard materials such as lentils and toroids together with a block matrix.

For the study, we used n-type silicon samples with an initial resistivity of $\rho = 15 \div 20 \Omega \cdot \text{cm}$.

Samples of n-Si<Ni> obtained by diffusion of nickel into single crystals of silicon, n-Si<Gd> - obtained by alloying during the growth of single crystals. Nickel diffusion and other technological cycles were carried out according to the procedure described in [3]. The samples obtained in this way were subjected all-round hydraulic pressure (ARHP) in the range $P = 1 \div 60$ kbar. At the same time, the geometric dimensions and

surface quality of the samples were identical. Before and after pressure relief and appropriate treatment, the IR transmission spectra of the samples were studied using the UR-20 infrared spectrometer. The concentrations of IR-active oxygen (N_O) and carbon (N_C) were determined from the magnitude of absorption peaks at $\lambda = 9,1 \mu\text{m}$ and $\lambda = 16,4 \mu\text{m}$, respectively, according to the formulas:

$$N_O = 4,8 \cdot 10^{17} \left(\frac{\alpha_1 d - \alpha_2 d}{d_0} \right) \quad (2)$$

$$N_C = 1,1 \cdot 10^{17} \left(\frac{\alpha d}{d_0} \right) \quad (3)$$

where, α – is the absorption coefficient, d_0 – is the thickness of the sample.

Studies have shown that in n-Si samples with $N_O \approx 8 \cdot 10^{17} \text{cm}^{-3}$ ARHP up to 40 kbar does not lead to a noticeable change in the peaks of oxygen and carbon absorption. At the same time, in n-Si<Ni> samples, it was found that after annealing at $P \geq 30$ kbar, the peaks of oxygen and carbon absorption gradually decrease and completely disappear at a pressure of $P = 55$ kbar (Table 1.).

Table 1. Concentration of optically active oxygen atoms at different pressure values

P, kbar	after T ₀ , T=1550K n-Si	n-Si <Ni>
0	$8 \cdot 10^{17} \text{cm}^{-3}$	$8 \cdot 10^{17} \text{cm}^{-3}$
4	$8 \cdot 10^{17} \text{cm}^{-3}$	$8 \cdot 10^{17} \text{cm}^{-3}$
8	$8 \cdot 10^{17} \text{cm}^{-3}$	$7,8 \cdot 10^{17} \text{cm}^{-3}$
12	$7,8 \cdot 10^{17} \text{cm}^{-3}$	$7,6 \cdot 10^{17} \text{cm}^{-3}$
16	$7,8 \cdot 10^{17} \text{cm}^{-3}$	$7,2 \cdot 10^{17} \text{cm}^{-3}$
20	$7,7 \cdot 10^{17} \text{cm}^{-3}$	$6,6 \cdot 10^{17} \text{cm}^{-3}$
30	$7,6 \cdot 10^{17} \text{cm}^{-3}$	$6,3 \cdot 10^{17} \text{cm}^{-3}$
40	$6,6 \cdot 10^{17} \text{cm}^{-3}$	$5,3 \cdot 10^{17} \text{cm}^{-3}$
50	$5,3 \cdot 10^{17} \text{cm}^{-3}$	$3,6 \cdot 10^{17} \text{cm}^{-3}$
55	$4,7 \cdot 10^{17} \text{cm}^{-3}$	$1,8 \cdot 10^{17} \text{cm}^{-3}$
60	$4,1 \cdot 10^{17} \text{cm}^{-3}$	$8,3 \cdot 10^{16} \text{cm}^{-3}$
65	$3,3 \cdot 10^{17} \text{cm}^{-3}$	–

In contrast to the samples with an admixture of nickel, the absorption spectra in the n-Si<Gd> samples turned out to be more sensitive to external pressure. As can be seen from Fig. 2, with an increase in the value of the external pressure from 20 kbar, the peak at $\lambda = 9,1 \mu\text{m}$ gradually decreases and at $P = 65$ kbar almost completely disappears.

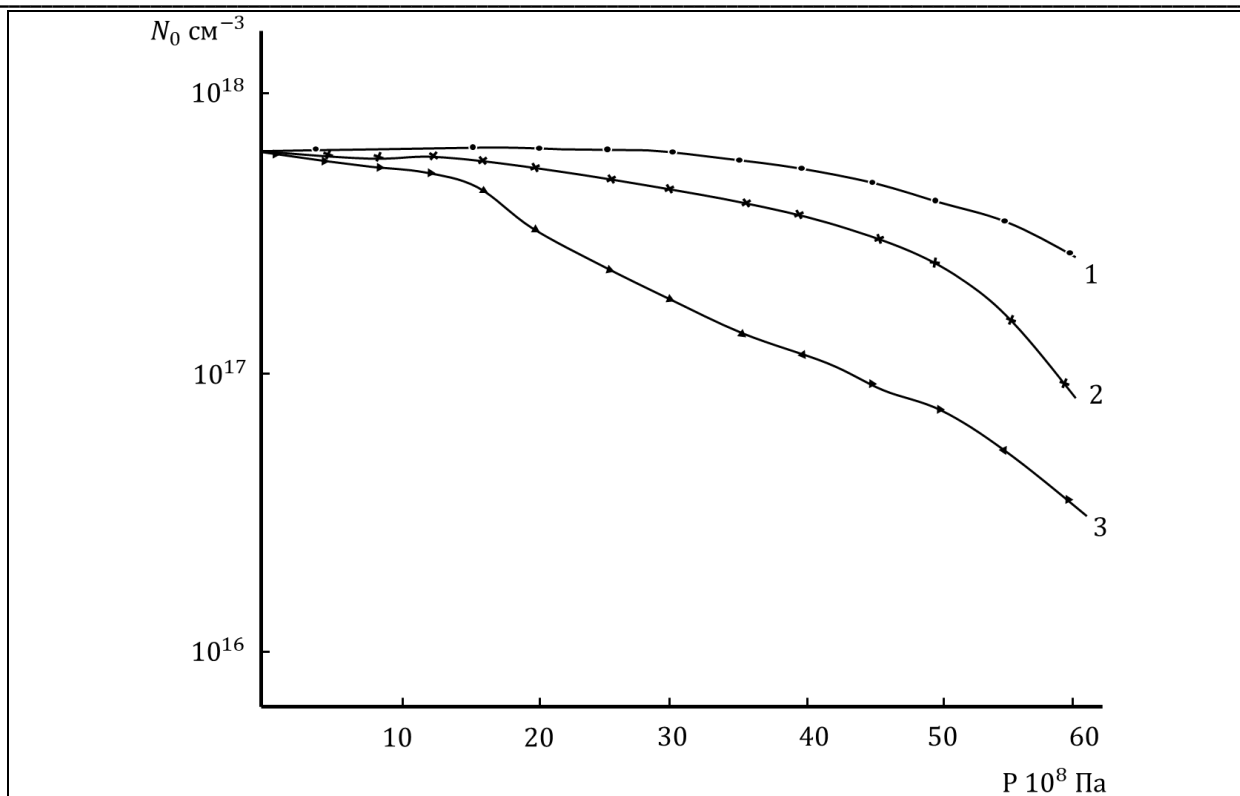


Fig. 2. Dependence of the concentration of optically active oxygen atoms on ARHP for n-Si samples (curve. 1), n-Si<Gd> (curve. 2), n-Si<Ni> (curve 3)

Comparing the curves of the absorption intensity dependence on P (Fig. 2), it can be seen that in n-Si<Gd> samples, the decrease in oxygen and carbon peaks begins at a pressure value of $P > 10$ kbar, when this P value for n-Si<Ni> is $P \geq 30$ kbar. We have carried out a qualitative assessment of the concentration of oxygen and carbon at different pressure values according to the formulas (2) and (3) which showed that at $P = 40$ kbar, the concentration of optically active oxygen atoms in n-Si<Ni> samples decreased to one order of magnitude relative to control samples. The concentration of optically active carbon atoms in these samples practically does not change in the pressure range $P = 1 \div 30$ kbar, and at $P = 35 \div 55$ kbar, a decrease in N_c by 45 ÷ 50% was found. Based on the results obtained, the dependence of changes in oxygen and carbon concentrations on pressure was calculated.

In works [5,6] the decay of impurity precipitates Ni and Gd under the action of external hydrostatic pressure, where it is shown that the defect formation energy of gadolinium precipitates is significantly less ($E_d^{Gd} \approx 2\text{eV}$) than the defect formation energy of nickel precipitates ($E_d^{Ni} \approx 4\text{eV}$). This means that the decay of gadolinium precipitates begins earlier than the decay of nickel precipitates when exposed to external pressure. It can be assumed that the increase in the concentration of oxygen atoms passing into an optically inactive state in n-Si<Ni> samples compared with n-Si is determined by its interaction with Ni and Gd atoms or their silicide formed after the decomposition of precipitates in the crystal volume.

Simultaneous changes in the resistivity and concentration of optically active oxygen and carbon atoms, in our opinion, are associated with the following processes:

1. With a high value of all-round hydrostatic pressure, the precipitates disintegrate simultaneously and new dislocation lines with various defects appear, which partially accelerates the disappearance of optically active oxygen atoms.
2. Formation of oxygen precipitation with the participation of carbon atoms.

Our experiments have shown that high hydrostatic pressure accelerates the precipitation of oxygen and carbon atoms. In this case, significant elastic stresses arise at the precipitate-matrix interface. With an increase in oxygen precipitation, the formation of complexes of the C_mO_m type proceeds.

Using the law of acting masses, E_a according to the formula:

$$[CO] \approx \exp(E_a/kT) \quad (5)$$

$E_a \approx 1,1$ eV was estimated.

It is assumed that with an increase in the values of the plastic deformation, the diffusion coefficient of oxygen atoms increases, which leads to their movement along dislocations, thereby disrupting the SiO_2 complex providing absorption of IR light at $\lambda = 9,1$ microns.

References:

1. V.M. Babich, N.I. Bletskan, E.F. Wenger. Oxygen in monocrystalline silicon, 1997
2. Yu.F. Shulpyakov, R.F. Vitman, A.N. Dremin, A.A. Lebedev. Effect of high pressure on the state of optically active oxygen in silicon during heat treatments Fiz. Tekh. Poluprov. -1984. -T. 18, V. 7. -p. 1306-1307
3. S.Z. Zainabidinov, P.I. Baranskiy, I.N. Karimov, A.R. Turaev and Kh. Kh. Karimberdiev. Effect of high hydrostatic pressure on the electrophysical properties of doped silicon crystals and devices based on them/ Solid-State Electronics Vol.38, No. 3. Pp. 693-695, 1995y.
4. J.Lang V.Sosnowska, Phil. Mag.50, 233(1984)
5. F.Kreger, Chemistry of Imperfect Crystals, Izd, Mir, Moscow 1969 (in Russia)
6. M. Lanno and K.Bourguin, Point defect in Semiconductors, Izd, Mir, Moscow 1984 (in Russia)
7. R.S.Antonenko, Yu.A.Karpov, V.I. Shakhavtsov, V.L.Shindich, L.I. Shpinar, and I.I. Yaskovets, Fiz. Tekh. Poluprov. 12, 1707 (1978)
8. S.P. Murarka(Ed). Silicides for VLSI Application. Academic Press. New York, 1963.